# Spatial micro-distribution of methanotrophic activity along a 120-year afforestation chronosequence

Karbin, Saeed ; Hagedorn, Frank ; Hiltbrunner, David ; Zimmermann, Stefan ; Niklaus, Pascal A

Abstract: Aims: Methanotrophic bacteria drive upland soil methane (CH4) uptake. Land-use change often affects their activity, but the mechanisms involved are not well understood. We studied soil-atmosphere CH4 fluxes along a 120-year Norway spruce afforestation chronosequence on subalpine pasture, testing whether effects were related to shifts in the spatial niche of methanotrophs. Previous field data had shown that soil 14CH4 uptake increased with forest age, and that this effect was driven by decreased water filled pore space due to higher rainfall interception in the more developed canopies of older forest stands. Methods: The spatial distribution of methanotrophic activity was determined by 14CH4-labelling followed by soil section preparation, aggregate size fractionation, aggregate erosion, and micro-autoradiographic imaging. Results: Uptake rates of CH4 measured in laboratory incubations of soil cores as well as their water contents largely followed the in situ measurements previously made in the field. 14CH4 assimilation was heterogeneously distributed, and occurred further down the soil profile in older forest that had a more developed organic layer that did not contribute to CH4 uptake. Assimilation was largest in 2—8 mm aggregates, and higher at the exterior than in the interior of aggregates. Conclusions: Our data indicates that differences in soil aggregation and related methanotrophic activities did not contribute substantially to higher CH4 uptake in older forest, mostly because aggregation did not change much with age. On a per mass basis, however, large aggregates contributed less to CH4 uptake due to their unfavorable surface to volume ratio. More generally, we argue that the (sub-)aggregate heterogeneity of soil microbial activity and diversity is underexplored, although it critically determines ecological interactions that drive ecosystem-level processes.

DOI: https://doi.org/10.1007/s11104-016-3141-5



Originally published at:
Karbin, Saeed; Hagedorn, Frank; Hiltbrunner, David; Zimmermann, Stefan; Niklaus, Pascal A (2017). Spatial micro-distribution of methanotrophic activity along a 120-year afforestation chronosequence. Plant and Soil, 415(1-2):13-23.
DOI: https://doi.org/10.1007/s11104-016-3141-5

# Spatial micro-distribution of methanotrophic activity along a 120-year afforestation chronosequence

Saeed Karbin[1], Frank Hagedorn[2], David Hiltbrunner[2], Stefan Zimmermann[2] and Pascal A. Niklaus[1]

*Plant and Soil*

First Online: 09 December 2016

DOI: 10.1007/s11104-016-3141-5

1) Institute of Evolutionary Biology and Environmental Studies, Winterthurerstrasse 190, CH-8057 Zürich, Switzerland

2) Swiss Federal Institute for Forest, Snow and Landscape Research WSL Zürcherstrasse 111, CH-8903, Birmensdorf, Switzerland

Correspondence: Pascal.Niklaus@ieu.uzh.ch

# Abstract

**Aims.** Methanotrophic bacteria drive upland soil methane ($CH_4$) uptake. Land-use change often affects their activity, but the mechanisms involved are not well understood. We studied soil-atmosphere $CH_4$ fluxes along a 120-year Norway spruce afforestation chronosequence on subalpine pasture, testing whether effects were related to shifts in the spatial niche of methanotrophs. Previous field data had shown that soil $^{14}CH_4$ uptake increased with forest age, and that this effect was driven by decreased water filled pore space due to higher rainfall interception in the more developed canopies of older forest stands.

**Methods.** The spatial distribution of methanotrophic activity was determined by $^{14}CH_4$-labelling followed by soil section preparation, aggregate size fractionation, aggregate erosion, and micro-autoradiographic imaging.

**Results.** Uptake rates of $CH_4$ measured in laboratory incubations of soil cores as well as their water contents largely followed the in situ measurements previously made in the field. $^{14}CH_4$ assimilation was heterogeneously distributed, and occurred further down the soil profile in older forest that had a more developed organic layer that did not contribute to $CH_4$ uptake. Assimilation was largest in 2—8 mm aggregates, and higher at the exterior than in the interior of aggregates.

**Conclusions.** Our data indicates that differences in soil aggregation and related methanotrophic activities did not contribute substantially to higher $CH_4$ uptake in older forest, mostly because aggregation did not change much with age. On a per mass basis, however, large aggregates contributed less to $CH_4$ uptake due to their unfavorable surface to volume ratio. More generally, we argue that the (sub-)aggregate heterogeneity of soil microbial activity and diversity is underexplored, although it critically determines ecological interactions that drive ecosystem-level processes.



**Keywords:** methanotrophic bacteria, soil aggregation, afforestation, $^{14}C$ labeling, land-use changes, spatial distribution of microbial activity

# Introduction

Anthropogenic activities including ruminant livestock farming, fossil fuel exploration, and rice cultivation have increased atmospheric methane ($CH_4$) concentrations above pre-industrial levels. $CH_4$ currently is the most important anthropogenic greenhouse gas after $CO_2$, with key components of the global $CH_4$ cycle being mediated by soil micro-organisms (IPCC, 2013). At low redox potential, e.g. in water-logged soils, methanogenic archaea produce $CH_4$. In contrast, oxic upland soils often are a net sink for atmospheric $CH_4$ due to the activity of methanotrophic bacteria. Methanotrophs can also oxidize $CH_4$ produced by soil-internal methanogenesis, so that they functionally act as a filter that reduces the amount of $CH_4$ that would otherwise be released to the atmosphere. Methanotrophic activity is environmentally beneficial because methanotrophs convert $CH_4$-carbon to organic forms or to $CO_2$ which has a much lower greenhouse warming potential than $CH_4$.

Upland soil often show no or only little methanogenesis, and $CH_4$ oxidation follows a "high affinity" kinetic. The nature of the methanotrophs driving the uptake of atmospheric $CH_4$ in these systems remains unclear, and methanotrophs able to grow under atmospheric $CH_4$ concentrations have not been isolated to date. DNA sequence data suggest that these are distinct from the communities found in systems with important soil-internal sources and thus periodically higher soil $CH_4$ concentrations (Dunfield, 2007), but recent studies have shown that flush feeders can temporally exhibit high-affinity kinetics (Baani and Liesack, 2008; Cai et al., 2016).

Irrespective of the identity of methanotrophs, $CH_4$ uptake by upland soils significantly changes with land-use. Forests generally oxidize larger amounts of atmospheric $CH_4$ than grassland (Boeckx et al., 1997; Gundersen et al., 2012; Tate et al., 2007), and $CH_4$ uptake by arable land often is even lower than in grassland (Barcena et al., 2014; Smith et al., 2000). As a general rule, conversion of forest to agricultural land reduces the soil $CH_4$ sink, whereas reverting arable or pasture systems back to forest increases soil $CH_4$ uptake (Menyailo et al., 2010; Menyailo and Hungate, 2003). Chronosequence and paired site studies suggest that the recovery of the soil $CH_4$ sink can take decades to centuries (Prieme et al., 1997; Smith et al., 2000), for reasons not well understood. Low recovery rates may be related to the presumably very slow growth rates of methanotrophic communities thriving mostly on

69 atmospheric $CH_4$, but indirect effects via nutrient dynamics or re-adjustments of soil structure may
70 also be at play (Conant et al., 2004; Duchicela et al., 2013; Spohn and Giani, 2011).

71 Several mechanisms have been proposed to explain the dependence of the soil $CH_4$ sink on land
72 use. First, the decline in $CH_4$ uptake in agricultural land may be related to the application of mineral
73 nitrogen fertilizers. In particular ammonium-based fertilizers have been shown to decrease soil $CH_4$
74 uptake (Hütsch et al., 1993), possibly by direct inhibition of $CH_4$ assimilation at the enzymatic level
75 (Carlsen et al., 1991; Dalton, 1977). While this mechanism has been demonstrated under laboratory
76 settings (Bedard and Knowles, 1989), it is less clear whether it also is responsible for such effects
77 under field conditions (e.g. Barcena et al., 2014; Bodelier and Laanbroek, 2004). Second, soil $CH_4$
78 sinks may also decrease in response to altered soil structure during land-use change (Abichou et al.,
79 2011; Ball et al., 1999; Hütsch, 1998). Soil properties such as water content, pore size distribution, and
80 gas diffusivity can alter methanotrophic activity and are related to soil aggregate structure (Kasper et
81 al., 2009). Methanotrophs have been shown to inhabit particular soil domains (Boeckx and van
82 Cleemput, 2001; Stiehl-Braun et al., 2011a), and soil $CH_4$ uptake can decline when aggregation is lost
83 (Abichou et al., 2011), suggesting that the ecological niches of methanotrophic bacteria are linked to
84 the occurrence of macro-aggregates. However, similar effects may also be due to a reduced number of
85 macro-pores and resulting higher water filled pore space, which likely limits diffusive methane
86 transport (Castro et al., 1994). In the long term, soil structural changes can also lead to shifts in
87 methanotrophic community composition (Kumaresan et al., 2011; McNamara et al., 2008; Singh et al.,
88 2007).

89 $CH_4$ uptake by soils may also vary at the sub-aggregate scale, e.g. radially within aggregates. The
90 exterior and interior of aggregates differ in physico-chemical characteristics and substrate availability,
91 thus providing distinct microhabitats for microbial communities (e.g. Wilcke et al., 1999). Using
92 microsensors, Hojberg et al. (1994) observed strong gradients in $O_2$ and $N_2O$ concentrations from the
93 surface to the core of soil aggregates. Based on $^{14}C$ imaging of assimilated $^{14}CH_4$ in soil cores
94 embedded in resin, Stiehl-Braun et al. (2011a) suggested that $CH_4$ uptake takes primarily place on
95 aggregate surfaces, but their results were inconclusive because aggregate surfaces could not
96 unequivocally be identified in their soil sections. However, this spatial niche would allow

97 methanotrophs the best access to atmospheric $CH_4$, but would expose them to more severe
98 environmental fluctuations (e.g. drought) and microbial grazing.

99 Given the extreme small-scale heterogeneity of upland soils, identifying the small-scale spatial
100 niche of methanotrophs is a key prerequisite to understand their ecology and to develop a mechanistic
101 understanding of microbial $CH_4$ transformations. To date, related investigations have been hindered
102 because tools allowing to study methanotrophic activity in a small-scale context are largely lacking, in
103 part because they cannot be cultivated and their nature thus remains in part elusive. We have
104 previously studied soil-atmosphere $CH_4$ flux rates in an afforestation chronosequence in which
105 Norway spruce (*Picea abies* L.) was established on a former subalpine pasture (Hiltbrunner et al.,
106 2012). Field-measured soil $CH_4$ uptake increased with stand age, and we speculated that these fluxes
107 were primarily driven by the volumetrically drier soils and decreased water filled pore space that we
108 had found. Here, we present further investigations in which we analyzed soil structural changes and
109 determined the spatial micro-distribution of soil $CH_4$ uptake. This was achieved by $^{14}CH_4$ labelling of
110 soil cores, followed by autoradiographic analysis of intact soil sections. We further physically
111 fractionated these soil cores and eroded aggregates to determine the spatial niche of the active
112 methanotrophs in relation to aggregate structure. We hypothesized aggregation would increase in older
113 forest stands, an effects that might be driven by larger soil carbon input rates and an increased
114 abundance of ectomycorrhizal fungi. At the micro-scale, we expected a distinct gradient of
115 methanotrophic activity within aggregates with the highest activity in the exterior of soil aggregates
116 due to larger $CH_4$ availability.

# Materials and Methods

## Site description

We studied the spatial distribution of methanotrophic activity along a sub-alpine afforestation chronosequence in Switzerland (Jaun pass area, Canton of Fribourg, 46°37'17 N; 7°15'54 E). The site is located on a south-facing slope extending from 1450 to 1700 m a.s.l. that has been used as pasture for probably several centuries but certainly for the past 150 years. After severe avalanches in 1956, an area of about 15 ha on the eastern part of the slope was gradually afforested with Norway spruce (*Picea abies* L.), while the western part remained as a pasture. Separate patches of forest were planted in different years, resulting in stands 25, 30, 40, 45, and >120 years old (see Hiltbrunner et al., 2012, for more details).

Soils are Eutric Cambisols on calcareous bedrock. On average, soils were 80 cm deep and carbonate-free to a depth of 60 cm. The mineral A horizon contained 18.7±2.1% sand, 31.2±0.7% silt (2—63 μm), and 50.1±1.8% clay (mean ± standard error of a total of 20 measurements). We refer to Hiltbrunner et al. (2013) for a more detailed description of the soil profile including the distribution of organic carbon. See Table 1 for climatic conditions.

## Soil sampling and $^{14}CH_4$ labelling

In September 2011 and again in September 2012, intact soil cores (20 cm depth x 6.5 cm internal diameter) were sampled in PVC tubes. Loose organic material, i.e. any $O_L$ horizon, was removed. We then pre-cut the top soil along the tube's circumference with a knife to minimize soil compaction and then drove the PVC tubes 15 cm into the soil. The A horizon was approximately 20 cm deep so that the cores covered $O_F$, $O_H$, and the top of the A horizon. The tubes were excavated from the side, capped at both ends to prevent water loss, and transported upright to the laboratory.

We incubated the soil cores (still capped at the bottom end) in air-tight 3 L jars. Soil net $CH_4$ uptake was determined by collecting three headspace samples at hourly intervals (Agilent 7890N gas chromatograph equipped with a flame ionisation detector, Wilmington, Delaware, USA). Soil-

atmosphere $CH_4$ flux rates were determined by linear regression of headspace concentrations vs. sampling time.

Thereafter, the jars were first ventilated for about 15 min and then radio-labelled by manually injecting $^{14}CH_4$ into the jars, in portions, using a syringe. We maintained headspace concentrations in the range of 5-8 µL $CH_4$ $L^{-1}$ (analysis by gas chromatography) for a total of 7 days. This was achieved by adding $^{14}CH_4$ when required. Once a total of ~100 kBq had been injected, we continued with the same procedure but adding unlabelled $CH_4$. The incubation jars also contained plastic tubes with 100 mL 1.5 M NaOH to prevent secondary fixation of $^{14}CO_2$ released by microbial respiration during the incubation. $O_2$ was regularly injected into the jars to maintain aerobic conditions (15–20% $O_2$).

## Autoradiographic imaging of intact soil cores

Two labeled soil cores per sampling date and plot were freeze-dried and impregnated with epoxy resin (Laromin C 260, BASF, Ludwigshafen, Germany, mixed at a ratio of 2:3 with Araldite DY 026SP hardener, Astorit AG, Einsiedeln, Switzerland). Resin penetration was improved by evacuating the soil cores with resin to an end pressure of 25 kPa, and slowly bringing the core back to atmospheric pressure. After about 2–3 d of curing at room temperature, the resin was fully hardened overnight at 60 °C. Then, the soil cores were cut twice length-wise and divided in three sections that were each mounted on 5×5 cm glass slides. The section's surfaces were leveled with a diamond cup mill (Discoplan, Struers GmbH, Birmensdorf, Switzerland) and used to expose phosphor imaging plates (BAS III S, Fuji Photo Film Ltd., Tokyo, Japan) for 3 d. The imaging plates were scanned by red-excited blue fluorescence at a resolution of 200 µm and the three slides representing a soil core recomposed using a Matlab-script that made use of the Image Processing Toolbox (Mathworks, Natick, MA). Recomposition was achieved by determining a transformation matrix (combination of translation and rotation) for each image part, based on the visual identification of control points that matched features opposite the line along which the slides had been separated. The label distribution was then explored visually and the vertical distribution of $^{14}C$ determined by averaging pixel intensities per horizontal pixel line. Areas with large stones were excluded for this procedure.

## Autoradiographic imaging of isolated soil aggregates

We isolated soil aggregates 2 to 12 mm in size from a separate labelled soil core per plot, attempting to minimize mechanical disturbance (September 28, 2011 sampling). These aggregates were placed in petri dishes and impregnated with epoxy resin as described previously for intact soil cores. Autoradiographies were obtained similarly.

## Aggregate fractionation

We eroded labeled soil aggregates mechanically to separate exterior and interior fractions slightly modifying the method described by Wilcke et al. (1999). First, labeled soil cores were divided into 0-6, 6-12 and 12-16 cm depth segments. Then, the soil depth segments were separated into aggregate size fractions (>16, 16-8, 8-4, 2-4, <2mm) by sieving through a series of sieves, applying only minimal mechanical energy. Each size fraction was weighed and its water content was determined gravimetrically (5 g subsample, 105°C). Approximately 300 g of soil aggregate size fractions were then frozen by immersion in liquid nitrogen. Then, material was eroded by repeated immersion in distilled water, which melted a thin layer on the outside of the aggregates, followed by shaking on a 2 mm sieve, which removed this layer. To erode approximately equal amounts of soil in each aggregate size fraction, the sieve was shaken 75, 60, 50 and 50 times for the >16, 16-8, 8-4 and 2-4 mm fraction, respectively. In the course of this procedure, aggregates dispersed from the exterior to the interior, with the eroded fractions collected in a water bowl underneath the sieve. The solid eroded material was obtained by transferring the suspension into a long glass tube adding a flocculation agent (2 mL 1 M $MgSO_4$) and pipetting the water above the settled soil material after 24 hours. All soil fractions were dried at 105°C. A subsample was ground in a mortar, oxidized (200 mg material, A307 sample oxidizer, Perkin Elmer, Waltham, MA) and its $^{14}C$ content determined by liquid scintillation counting (TRI-2900TR, Perkin Elmer, Waltham, MA). Soluble $^{14}C$ remaining in the supernatant of the solution used for aggregate erosion was determined similarly (Ultima Gold scintillation cocktail, Perklin Elmer).

## Statistical analysis

Data were analyzed by fitting linear models reflecting the design of the study. We fitted effects of land use type (forest vs. grassland), forest stand age (log-transformed), and altitude. Since altitude and stand age were not orthogonal (Hiltbrunner et al., 2012), we fitted models correcting for altitude-effects before and after stand age to estimate the degree of confounding. When several measures per plot were analyzed (e.g. repeated measures or analyses including several soil layers), linear mixed effects models were fitted (ASReml, VSN International, Hempel-Hempstead, UK) which included the additional random effects plot, and, where appropriate, plot × year. These terms are necessary to ensure proper replication of significance tests. For the analysis of activity by soil layer, data were averaged by 1 cm soil layers and a first order autoregressive spatial correlation structure between soil layers included in the analysis to account for non-independence of residuals from the same soil core and plot.

205 # Results

206 ## $CH_4$ uptake by soil cores

207 Net $CH_4$ uptake of soil cores did not differ significantly between grassland and forest, but
208 increased with forest stand age (Fig. 1, linear model correcting for altitude; P=0.06 for joint analysis of
209 both years; P=0.03 when 2012 data analyzed separately; n.s. for 2011). Volumetric soil moisture was
210 significantly higher in pasture than in forest soil (Fig. 2, P<0.01, joint analysis for both years), but no
211 effect of forest age was detected.

212 ## $^{14}CH_4$ assimilation in soil aggregate fractions

213 The soils investigated were well-aggregated, with 10% of the soil material recovered in the
214 <2mm fraction, 20% in both the 2-4 and 4-8 mm fraction, 38% in the 8-16 mm fraction, and 11% in
215 the >16mm fraction (Fig. 3). The size of the largest fraction was sensitive to soil handling during the
216 sieving process and more variable; the statistical analyses were therefore restricted to the small
217 fractions. Average aggregate size increased with depth, both in grassland and forest (P<0.001 for size
218 × depth), and decreased with forest stand age (P=0.02 for size × age), and more so in deeper soil layers
219 (P<0.01 for size × age × depth).

220 The concentrations of $^{14}C$, reflecting net $^{14}CH_4$ assimilation, were generally higher in small than
221 in large aggregates (Table 1; P<0.001), irrespective of land use, forest age, and soil depth.
222 Nevertheless, a larger total fraction of the applied label was found in larger aggregate classes because
223 these made up a larger mass fraction (Table 2). The eroded exterior of the aggregates contained
224 approximately twice as much $^{14}C$ per unit mass than the stable interior in all aggregate classes (Fig. 4).

225 ## Spatial distribution of $^{14}C$ in soil sections

226 Net assimilation of $^{14}C$ in soil was heterogeneous (Figs. 5 and 6), with increased activities on the
227 surface of aggregates. While aggregate surfaces are difficult to identify in intact sections, this finding
228 was confirmed by the autoradiographies of isolated aggregates (Fig. 7). The $^{14}C$-depth profiles differed
229 between grassland and forest (Fig. 8, P<0.001), with mean $^{14}CH_4$ assimilation depth (i.e. depth

230 weighted by $^{14}C$ content) about 1 cm closer to the soil surface in grassland ($P<0.01$). Within the forest
231 plots, the amount of $^{14}C$ assimilated in the layers near the soil surface decreased with stand age (Figs.
232 5 and 6; $P<0.05$ for layer × age), and mean $^{14}C$ depth therefore increased with age ($P<0.05$).

## Discussion

Along the afforestation chronosequence investigated here, we have measured soil-atmosphere fluxes of $CH_4$ in a previous study (Hiltbrunner et al., 2012) and found that net soil $CH_4$ uptake increased with forest stand age and that this effect correlated negatively with soil moisture and water filled pore space. Bulk density and soil porosity did not explain this pattern, and we concluded that the observed increase in soil $CH_4$ uptake was most likely driven by higher rainfall interception in the older forest canopies (Hiltbrunner et al., 2012). However, soil $CH_4$ fluxes are also affected by a multitude of other drivers which are frequently linked to soil structure (Hütsch, 1998; Shukla et al., 2013). Our $^{14}C$ based analysis of the micro-scale distribution of methanotrophic activity revealed a heterogeneous distribution in soils, with higher activities at the exterior than in the interior of soil aggregates. The active $CH_4$-assimilating zone shifted downwards the soil profile with increasing stand age; this effect was due to the development of an organic layer ($O_F$ and $O_H$ horizon) that did not contribute to $CH_4$ uptake.

Soil-atmosphere fluxes of trace gases are difficult to measure under laboratory conditions, and often deviate from in-situ assessments (Abichou et al., 2011; Hiltbrunner et al., 2012). Reasons include altered environmental conditions (e.g. temperature profiles and gas transport), effects of disturbance (e.g. compaction, removal of live plant roots), and in the case of soil cores also edge effects (e.g. facilitated diffusion along the core walls). Our laboratory incubations were therefore not intended as substitute for field measurements but to confirm that conditions largely reflected the patterns we had found in the field one year before (Hiltbrunner et al., 2012). The observed increases in $CH_4$ oxidation in forest relative to grassland are in agreement with the findings in temperate pine (Peichl et al., 2010) and hardwood forests (Menyailo and Hungate, 2003), but in contrast to Christiansen and Gundersen (2011) who reported decreasing $CH_4$ uptake in spruce forest. In a Danish 200-year chronosequence of oak and larch, Barcena et al. (2014) found increasing abundances of methane oxidizing soil bacteria with stand age. In our study, methanotrophic activity shifted downwards with forest soil development, an effect that is most likely related to the buildup of an organic layer which showed no substantial $CH_4$ oxidation. This finding is compatible with other

studies in which $CH_4$ oxidation was low or absent in the organic layer and concentrates in the top layers of the mineral soils (e.g. Adamsen and King, 1993; Bradford et al., 2001). Also, methanotrophic activity can be inhibited by monoterpenes (Amaral et al., 1998) and organic acids (Wieczorek et al., 2011), processes which may be more important in the organic layer of mature forest stands. Oxidation rates of atmospheric $CH_4$ generally are limited by diffusion rates due to the low $CH_4$ concentrations; a downward shift of activity thus would tend to decrease soil $CH_4$ uptake rates. In the present study, however, such an effect was not evident, probably because the diffusive resistance of the relatively well-aerated organic layer was low. This situation is comparable to the findings of Stiehl-Braun et al. (2011a) who reported that fertilizer application inhibited methanotrophic activity in top soil layers of a grassland but that the inhibition had no effect on soil-atmosphere $CH_4$ exchange – at least when soils were dry. In the afforestation chronosequence we studied, soils in older forest stands also were drier because the taller forest canopies intercepted more rainfall and the organic layer had a greater pore space. Therefore, if there would have been a limiting effect of the downward shift in methanotrophic activity, it might have been compensated by a lower soil moisture and a greater $CH_4$ diffusion into the mineral soil.

Several studies reported a relation between soil $CH_4$ uptake and nitrification. For example, Reay et al. (2005) found low $CH_4$ uptake in the top organic layer of Alder stands. Low $CH_4$ oxidation was associated with high nitrification rates. $CH_4$ oxidation rates were higher and nitrification rates lower in stands of other species, including Norway spruce, the species planted in our study. Potential nitrification rates generally are largest near the surface of forest soils, and generally decrease with depth (Laverman et al., 2000). How this relates to the inhibition of high affinity $CH_4$ oxidation is more complicated, because nitrification on one hand removes $NH_4^+$ (or $NH_3$), a compound known to inhibit $CH_4$ oxidation by competing for the active site of methane mono-oxygenase, but on the other hand nitrification often is an indication of high $NH_4^+$ concentrations, even if these are not found in bulk soil measurements because these are restricted to episodic events or small domains within soil structure. Also, intermediate products of nitrification (e.g. $NO_2^-$) may have detrimental effects on methanotrophs (King and Schnell, 1994; Schnell and King, 1994). Finally, mineral N concentrations sometimes also are positively correlated to the soil $CH_4$ sink (Bodelier and Laanbroek, 2004). We do not have a

288 detailed analysis of nitrogen cycling for our site; however, at our site, Hiltbrunner et al. (2012) did not
289 find changes in nitrification rates with forest stand age, and it therefore appears unlikely that
290 nitrification was an important driver of the age effects we observed.

291 Small-scale heterogeneity in soil methanotrophic activity has been reported in previous studies
292 that adopted autoradiographic techniques (Karbin et al., 2015a; Karbin et al., 2015b; Rime and
293 Niklaus, 2017; Stiehl-Braun et al., 2011a; Stiehl-Braun et al., 2011b). While we have argued that this
294 heterogeneity was related to aggregate structure, soil structure was not unambiguously identifiable
295 once the soil cores were embedded in resin. The enhanced activities in eroded aggregate surfaces now
296 demonstrate that indeed methanotrophic activity is concentrated in the aggregate's exterior and is
297 largely absent in their center. Very likely, this pattern can be attributed to diffusion limitations
298 (Hojberg et al., 1994). On the other hand, locations towards the aggregate core would protect
299 methanotrophs from adverse biotic and abiotic effects such as protozoan grazing, drought stress,
300 freeze-thaw events, and possibly also chemical inhibition by organic compounds such as terpenes
301 (Amaral et al., 1998). Such adverse effects could be important given the oligotrophic nature of
302 methanotrophs in low $CH_4$ environments which implies a low resilience after disturbance.

303 We found the largest concentrations of label from $^{14}CH_4$ assimilation in the smalles aggregates,
304 irrespective of forest age. As soil aggregate volume increases, air diffusion into the central part of soil
305 aggregate decreases (Sexstone et al., 1985), and $CH_4$ availability will become restricted. Small
306 aggregates have a larger surface to volume ratio, which may explain why the $^{14}C$ label decreased with
307 size. In our study, comparing aggregation among forest ages was difficult because we sampled by
308 depth rather than by horizon. However, our data suggest that aggregation did not change much with
309 age. In other studies, increasing fractions of macro-aggregates were found under afforestation (Wei et
310 al., 2013; Wu et al., 2013), but these studies focused on much smaller aggregates (macro aggregates
311 were defined as exceeding a diameter of 0.25 mm) and soils had a long history of tillage. Interestingly,
312 aggregates smaller than 2 mm showed lower $^{14}CH_4$ uptake in our study.

313 In conclusion, our results indicate an increased soil $CH_4$ uptake in older forest stands, which can
314 be related to lower soil moisture due to interception and possibly also to a larger share of aggregates
315 showing a higher than average methanotrophic activity. Our analysis of aggregate sizes and fractions

316 indicates small-scale heterogeneity in the distribution of methanotrophic activity that follows a radial
317 gradient with the highest activities at the exterior of aggregates. It would be promising to analyze,
318 using molecular methods, whether this gradient in activity coincides with a gradient in methanotrophic
319 abundance. More generally, the small-scale (sub-aggregate) spatial heterogeneity of soil microbial
320 activity and diversity currently appears underexplored, although it may have important implications
321 for our understanding of the ecological mechanisms that control microbially-mediated processes at the
322 ecosystem-level.

## Acknowledgements

We gratefully acknowledge Patrick Schleppi for field and laboratory assistance. This study was funded by the University of Zurich and a stipend of the Aga Khan Foundation to SK.

# Tables

**Table 1**. Climatic conditions at the field site. Data are monthly means and their standard deviations for the 1960-2012 period, for an elevation of 1650 m a.s.l. Data were interpolated based on data from a network of climate stations that was combined with simulations using a regional climate model (see Remund et al., 2016) for further details).

| Month | Temperature (°C) | Precipitation (mm) |
|---|---|---|
| Jan | -2.6 ± 2.4 | 101 ± 71 |
| Feb | -2.6 ± 2.7 | 99 ± 71 |
| Mar | -0.6 ± 2.2 | 103 ± 62 |
| Apr | 2.3 ± 1.9 | 98 ± 46 |
| May | 6.8 ± 1.8 | 119 ± 42 |
| Jun | 10.0 ± 1.6 | 143 ± 51 |
| Jul | 12.2 ± 1.5 | 147 ± 51 |
| Aug | 12.0 ± 1.6 | 151 ± 51 |
| Sep | 9.3 ± 1.8 | 103 ± 48 |
| Oct | 6.0 ± 2.0 | 96 ± 58 |
| Nov | 0.9 ± 2.1 | 111 ± 73 |
| Dec | -1.8 ± 2.2 | 124 ± 78 |

334 **Table 2**. Amount of label recovered in aggregate size fractions, expressed as total activity and
335 concentration per dry aggregate mass. Note that the largest fraction is not well defined (see methods
336 for details).

| Size class | $^{14}$C label | |
|---|---|---|
| | total (Bq) | concentration (Bq g$^{-1}$) |
| >16 mm | 31639 ± 6555 | 481 ± 46 |
| 8-16 mm | 62816 ± 11282 | 589 ± 36 |
| 4-8 mm | 36723 ± 5497 | 655 ± 41 |
| 2-4 mm | 44857 ± 6549 | 760 ± 49 |
| 0-2 mm | 21097 ± 1951 | 931 ± 61 |

337

# Figures

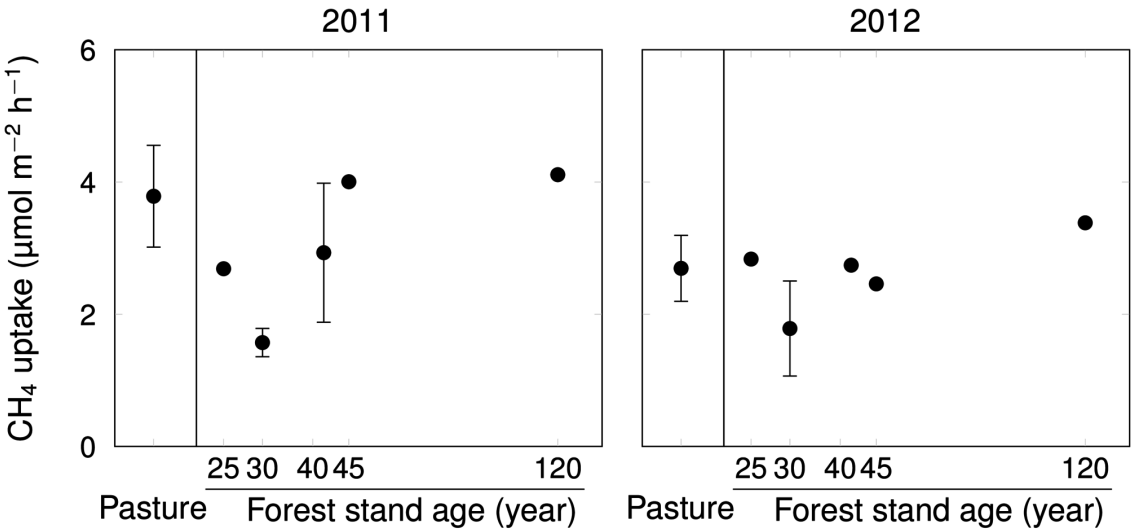


Figure 1: Net $CH_4$ uptake of soil cores collected on September 28, 2011 (left) and September 28, 2012 (right), in dependence of land use (pasture vs forest) and stand age (forest only). Error bars indicate standard errors.

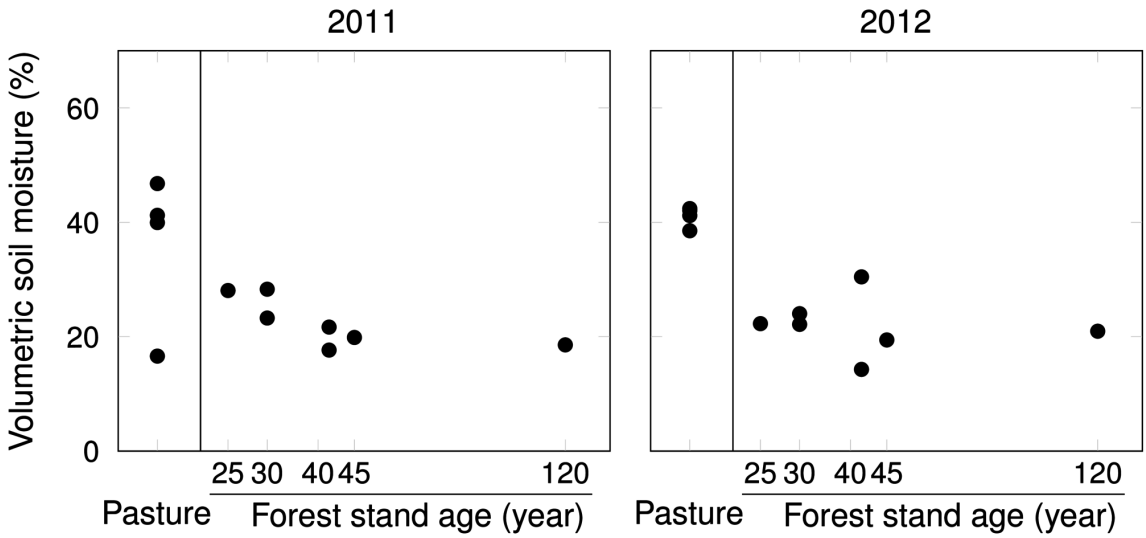


344

345 Figure 2: Volumetric soil moisture in soil cores collected on September 28, 2011 (left) and September

346 28, 2012 (right), in dependence of land use (pasture vs forest) and stand age (forest only).

347

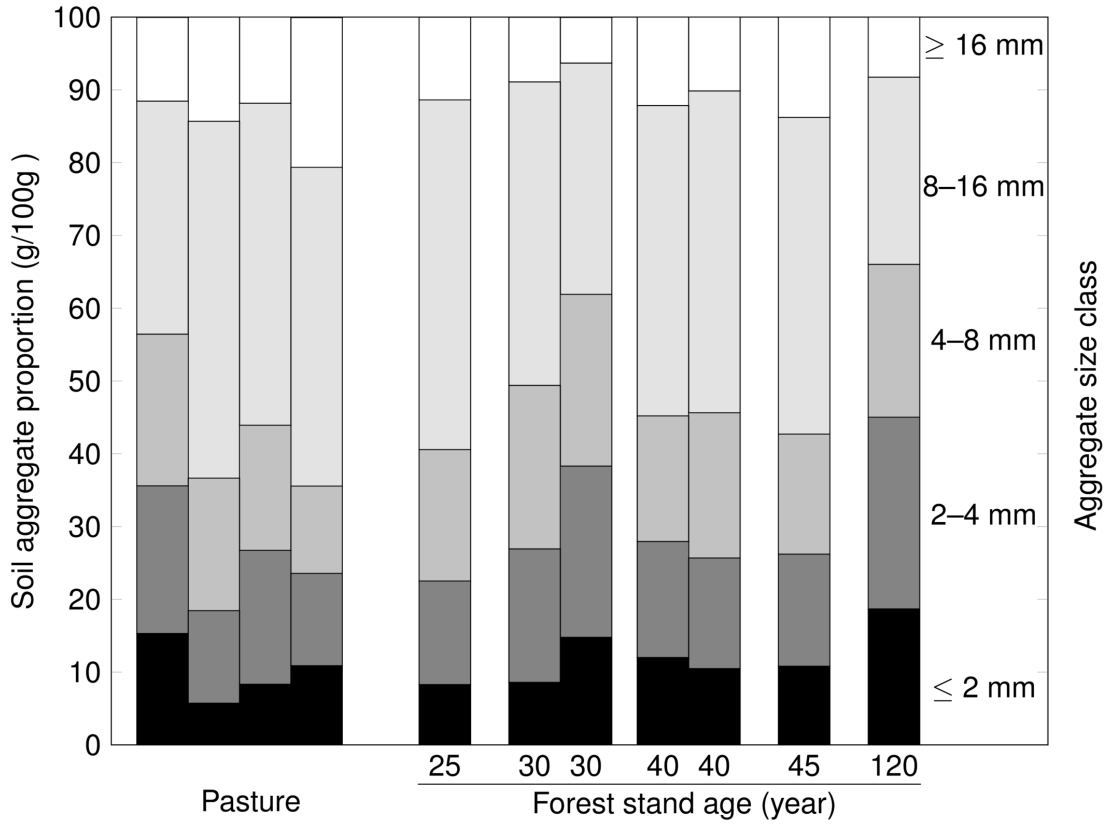


348

349 Figure 3: Soil aggregate size distribution in pasture and forest plots. Data are shown for each
350 fractionated soil core separately. Bars indicate the average fraction across the three depth layers
351 analyzed (0-6, 6-12, 12-18 cm).

352

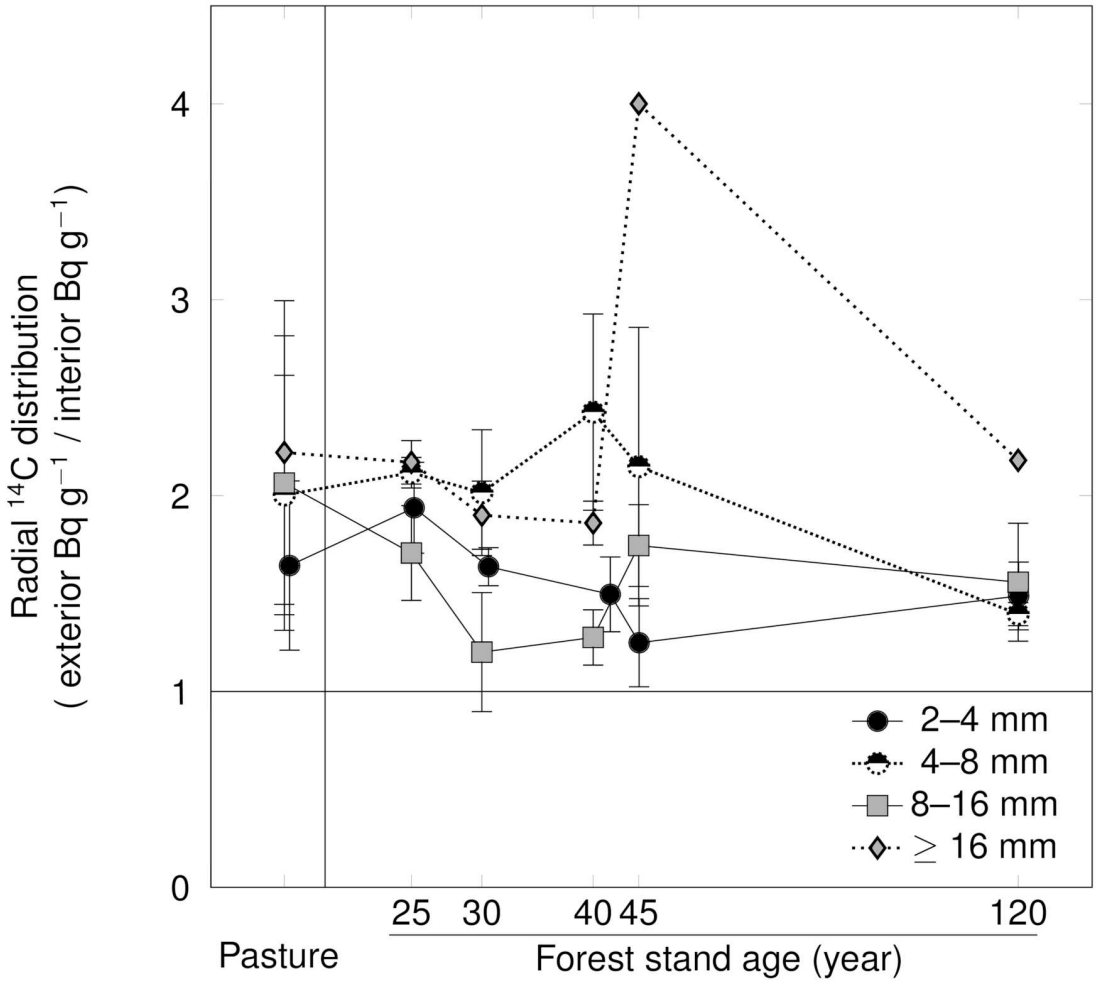


353

354 Figure 4: Ratio of $^{14}$C concentration in the eroded exterior part of aggregates relative to the
355 concentration in the remaining interior part, in dependence of land use, forest stand age, and aggregate
356 size class. Data are means ± standard errors, using plots as replicate.

357

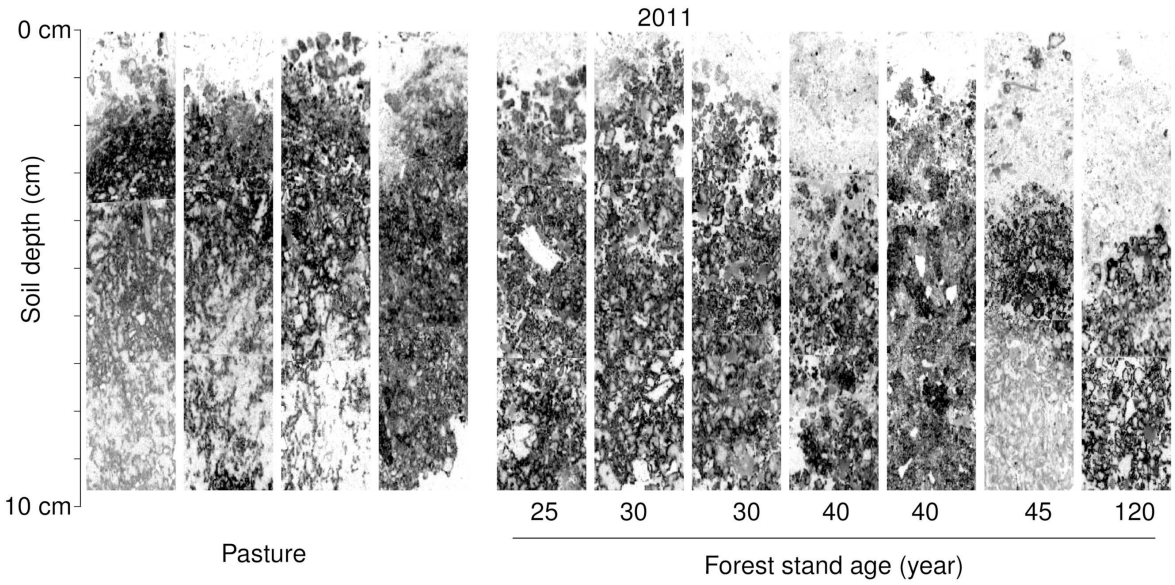


358

359 Figure 5: Auto-radiographic image of soil cores harvested on September 28 2011. Darker pixels
360 indicate stronger $^{14}C$ labelling. Note that these images show the relative label distribution within
361 individual soil cores. Differences in $CH_4$ uptake rate among cores are not visible because the cores
362 were labelled separately, each with an approximately equal amount of $^{14}C$.

363

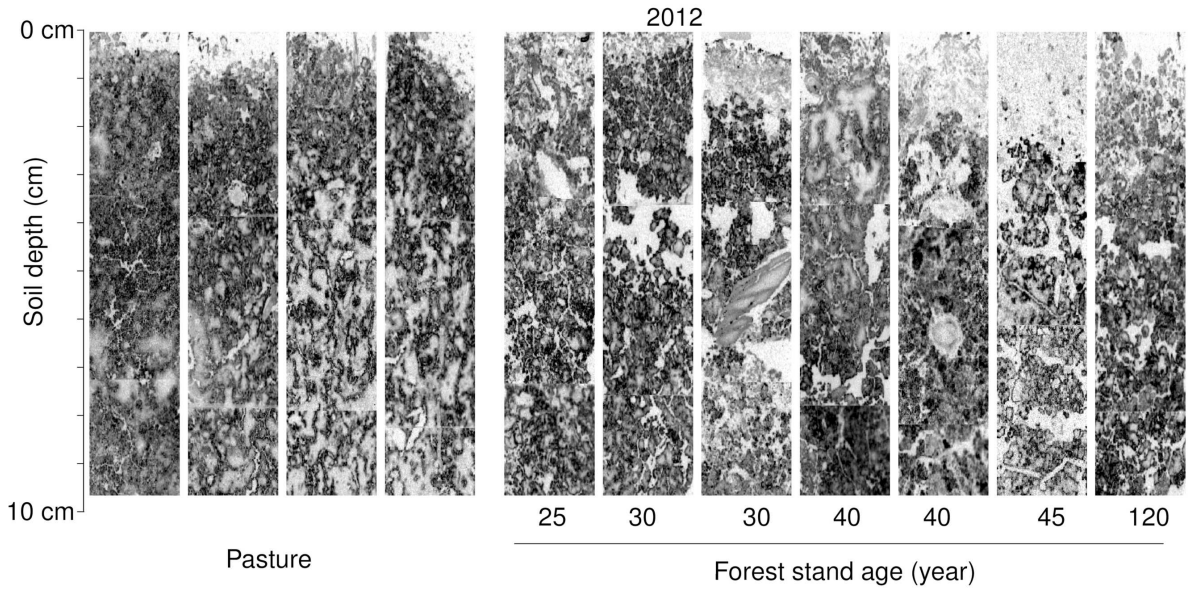


364

365 Figure 6: Auto-radiographic image of soil cores harvested on September 28 2012. Darker pixels
366 indicate stronger $^{14}C$ labelling. See legend of Fig. 5 for details.

367

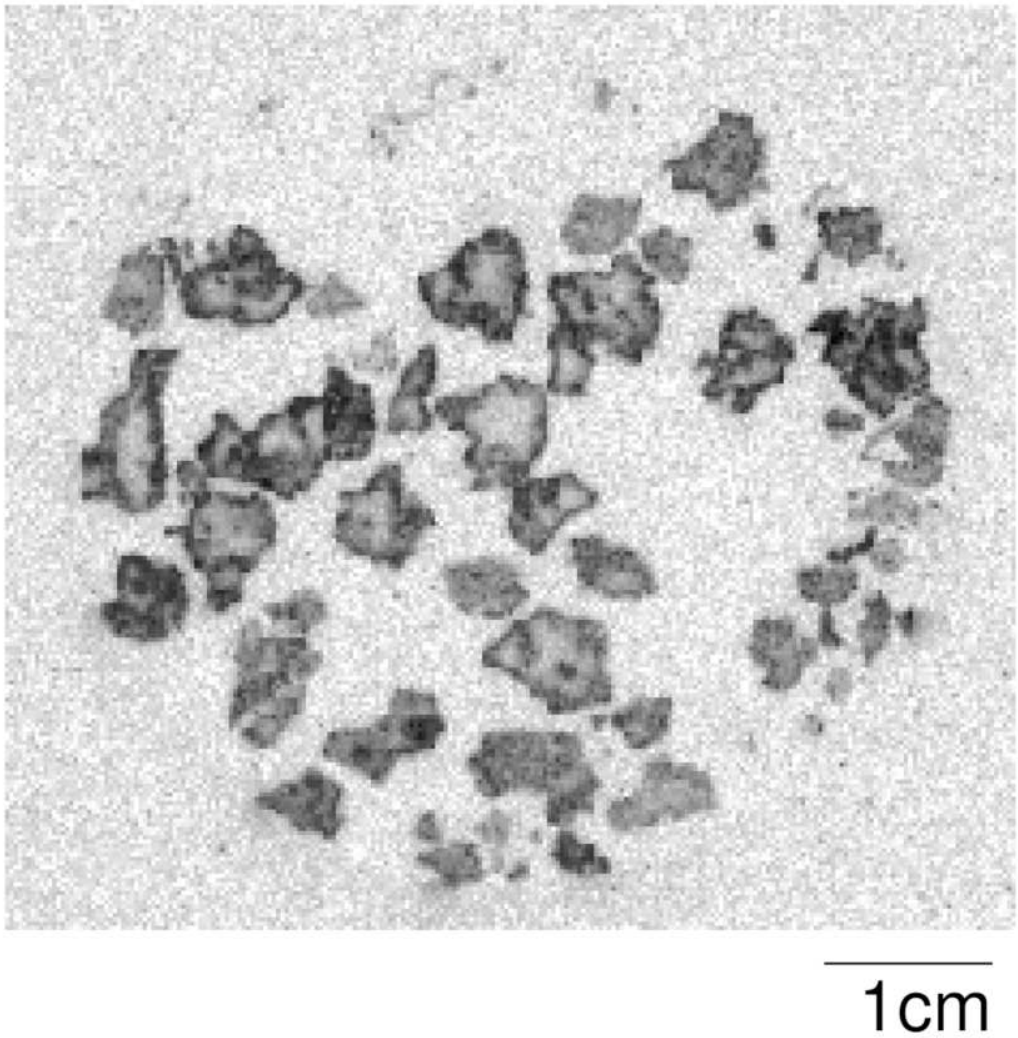


368

369 Figure 7: Auto-radiographic images of soil aggregates. Darker pixels indicate higher amounts of

370 assimilated $^{14}C$.

371

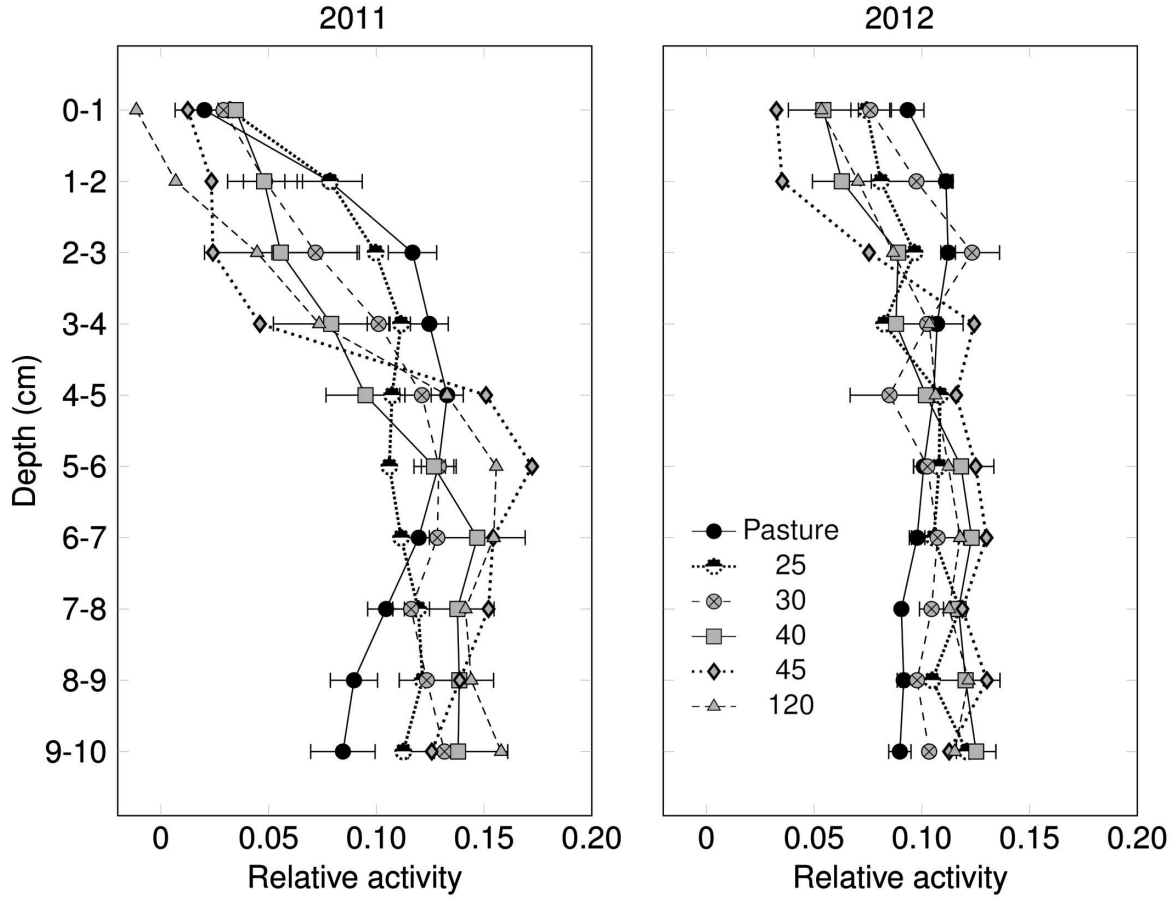


372

373 Figure 8: Depth distribution of net $^{14}CH_4$ assimilation in soil cores harvested on September 28, 2011
374 (left) and September 28, 2012 (right). Activities were standardized core-wise to unity sum of all 1 cm-
375 layers. Data shown are means ± 1 s.e., using plots as replicates.

376

# References


Abichou, T., Mahieu, K., Chanton, J., Romdhane, M., Mansouri, I., 2011. Scaling methane oxidation: From laboratory incubation experiments to landfill cover field conditions. Waste Management 31, 978-986.

Adamsen, A.P.S., King, G.M., 1993. Methane consumption in temperate and sub-arctic forest soils - rates, vertical zonation, and responses to water and nitrogen. Applied and Environmental Microbiology 59, 485-490.

Amaral, J.A., Ekins, A., Richards, S.R., Knowles, R., 1998. Effect of selected monoterpenes on methane oxidation, denitrification, and aerobic metabolism by bacteria in pure culture. Applied and Environmental Microbiology 64, 520-525.

Baani, M., Liesack, W., 2008. Two isozymes of particulate methane monooxygenase with different methane oxidation kinetics are found in *Methylocystis* sp. strain SCZ. Proceedings of the National Academy of Sciences of the United States of America 105, 10203-10208.

Ball, B.C., Scott, A., Parker, J.P., 1999. Field $N_2O$, $CO_2$ and $CH_4$ fluxes in relation to tillage, compaction and soil quality in Scotland. Soil & Tillage Research 53, 29-39.

Barcena, T.G., D'Imperio, L., Gundersen, P., Vesterdal, L., Prieme, A., Christiansen, R., 2014. Conversion of cropland to forest increases soil $CH_4$ oxidation and abundance of $CH_4$ oxidizing bacteria with stand age. Applied Soil Ecology 79, 49-58.

Bedard, C., Knowles, R., 1989. Physiology, biochemistry, and specific inhibitors of $CH_4$, $NH_4^+$, and CO oxidation by methanotrophs and nitrifiers. Microbiological Reviews 53, 68-84.

Bodelier, P.L.E., Laanbroek, H.J., 2004. Nitrogen as a regulatory factor of methane oxidation in soils and sediments. FEMS Microbiology Ecology 47, 265-277.

Boeckx, P., van Cleemput, O., 2001. Estimates of $N_2O$ and $CH_4$ fluxes from agricultural lands in various regions in Europe. Nutrient Cycling in Agroecosystems 60, 35-47.

Boeckx, P., van Cleemput, O., Villaralvo, I., 1997. Methane oxidation in soils with different textures and land use. Nutrient Cycling in Agroecosystems 49, 91-95.

Bradford, M.A., Ineson, P., Wookey, P.A., Lappin-Scott, H.M., 2001. Role of $CH_4$ oxidation, production and transport in forest soil $CH_4$ flux. Soil Biology & Biochemistry 33, 1625-1631.

Cai, Y.F., Zheng, Y., Bodelier, P.L.E., Conrad, R., Jia, Z.J., 2016. Conventional methanotrophs are responsible for atmospheric methane oxidation in paddy soils. Nature Communications 7:11728.

Carlsen, H.N., Joergensen, L., Degn, H., 1991. Inhibition by ammonia of methane utilization in *Methylococcus Capsulatus* (Bath). Applied Microbiology and Biotechnology 35, 124-127.

Castro, M.S., Melillo, J.M., Steudler, P.A., Chapman, J.W., 1994. Soil moisture as a predictor of methane uptake by temperate forest soils. Canadian Journal of Forest Research 24, 1805-1810.

Christiansen, J.R., Gundersen, P., 2011. Stand age and tree species affect $N_2O$ and $CH_4$ exchange from afforested soils. Biogeosciences 8, 2535-2546.

Conant, R.T., Six, J., Paustian, K., 2004. Land use effects on soil carbon fractions in the southeastern United States. II. Changes in soil carbon fractions along a forest to pasture chronosequence. Biology and Fertility of Soils 40, 194-200.

Dalton, H., 1977. Ammonia oxidation by the methane oxidising bacterium *Methylococcus capsulatus* strain Bath. Archives of Microbiology 114, 273-279.

Duchicela, J., Sullivan, T.S., Bontti, E., Bever, J.D., 2013. Soil aggregate stability increase is strongly related to fungal community succession along an abandoned agricultural field chronosequence in the Bolivian Altiplano. Journal of Applied Ecology 50, 1266-1273.

Dunfield, P.F., 2007. The soil methane sink, In: Reay, D.S., Hewitt, C.N., Smith, K.A., Grace, J. (Eds.), Greenhouse Gas Sinks. CABI publishing, Oxon, UK, pp. 152-170.

Gundersen, P., Christiansen, J.R., Alberti, G., Bruggemann, N., Castaldi, S., Gasche, R., Kitzler, B., Klemedtsson, L., Lobo-do-Vale, R., Moldan, F., Rutting, T., Schleppi, P., Weslien, P., Zechmeister-Boltenstern, S., 2012. The response of methane and nitrous oxide fluxes to forest change in Europe. Biogeosciences 9, 3999-4012.

Hiltbrunner, D., Zimmermann, S., Hagedorn, F., 2013. Afforestation with Norway spruce on a subalpine pasture alters carbon dynamics but only moderately affects soil carbon storage. Biogeochemistry 115, 251-266.

Hiltbrunner, D., Zimmermann, S., Karbin, S., Hagedorn, F., Niklaus, P.A., 2012. Increasing soil methane sink along a 120-year afforestation chronosequence is driven by soil moisture. Global Change Biology 18, 3664-3671.

Hojberg, O., Revsbech, N.P., Tiedje, J.M., 1994. Denitrification in soil aggregates analyzed with microsensors for nitrous oxide and oxygen. Soil Science Society of America Journal 58, 1691-1698.

Hütsch, B.W., 1998. Tillage and land use effects on methane oxidation rates and their vertical profiles in soil. Biology and Fertility of Soils 27, 284-292.

Hütsch, B.W., Webster, C.P., Powlson, D.S., 1993. Long-term effects of nitrogen fertilization on methane oxidation in soil of the Broadbalk Wheat Experiment. Soil Biology & Biochemistry 25, 1307-1315.

IPCC, 2013. Climate change 2013: the physical science basis, Fifth assessment report of the intergovernmental panel on climate change. Cambridge University Press, UK and USA, 1552 pp.

Karbin, S., Guillet, C., Kammann, C.I., Niklaus, P.A., 2015a. Effects of long-term $CO_2$ enrichment on soil-atmosphere CH4 fluxes and the spatial micro-distribution of methanotrophic bacteria. PLoS one 10, e0131665.

Karbin, S., Hagedorn, F., Dawes, M.A., Niklaus, P.A., 2015b. Treeline soil warming does not affect soil methane fluxes and the spatial micro-distribution of methanotrophic bacteria. Soil Biology & Biochemistry 86, 164-171.

449 Kasper, M., Buchan, G.D., Mentler, A., Blum, W.E.H., 2009. Influence of soil tillage systems on
450 aggregate stability and the distribution of C and N in different aggregate fractions. Soil & Tillage
451 Research 105, 192-199.
452 King, G.M., Schnell, S., 1994. Ammonium and nitrite inhibition of methane oxidation by
453 *Methylobacter Albus* Bg8 and *Methylosinus Trichosporium* Ob3b at low methane concentrations.
454 Applied and Environmental Microbiology 60, 3508-3513.
455 Kumaresan, D., Stralis-Pavese, N., Abell, G.C.J., Bodrossy, L., Murrell, J.C., 2011. Physical
456 disturbance to ecological niches created by soil structure alters community composition of
457 methanotrophs. Environmental Microbiology Reports 3, 613-621.
458 Laverman, A.M., Zoomer, H.R., Engelbrecht, D., Berg, M.P., van Straalen, N.M., van Verseveld,
459 H.W., Verhoef, H.A., 2000. Soil layer-specific variability in net nitrification and denitrification in
460 an acid coniferous forest. Biology and Fertility of Soils 32, 427-434.
461 McNamara, N.P., Black, H.I.J., Piearce, T.G., Reay, D.S., Ineson, P., 2008. The influence of
462 afforestation and tree species on soil methane fluxes from shallow organic soils at the UK
463 Gisburn Forest Experiment. Soil Use and Management 24, 1-7.
464 Menyailo, O.V., Abraham, W.R., Conrad, R., 2010. Tree species affect atmospheric $CH_4$ oxidation
465 without altering community composition of soil methanotrophs. Soil Biology & Biochemistry 42,
466 101-107.
467 Menyailo, O.V., Hungate, B.A., 2003. Interactive effects of tree species and soil moisture on methane
468 consumption. Soil Biology & Biochemistry 35, 625-628.
469 Peichl, M., Arain, M.A., Ullah, S., Moore, T.R., 2010. Carbon dioxide, methane, and nitrous oxide
470 exchanges in an age-sequence of temperate pine forests. Global Change Biology 16, 2198-2212.
471 Prieme, A., Christensen, S., Dobbie, K.E., Smith, K.A., 1997. Slow increase in rate of methane
472 oxidation in soils with time following land use change from arable agriculture to woodland. Soil
473 Biology & Biochemistry 29, 1269-1273.
474 Reay, D.S., Nedwell, D.B., McNamara, N., Ineson, P., 2005. Effect of tree species on methane and
475 ammonium oxidation capacity in forest soils. Soil Biology & Biochemistry 37, 719-730.
476 Remund, J., Rihm, B., Huegenin-Landl, B., 2016. Klimadaten für die Waldmodellierung für das 20.
477 und 21. Jahrhundert. Schlussbericht des Projektes im Forschungsprogramm Wald und
478 Klimawandel. Eidg. Forschungsanstalt für Wald, Schnee und Landschaft WSL., 39pp,
479 DOI:10.3929/ethz-a-010693673.
480 Rime, T., Niklaus, P.A., 2017. Spatio-temporal dynamics of soil $CH_4$ uptake after application of N
481 fertilizer with and without the nitrification inhibitor 3,4-dimethylpyrazole phosphate (DMPP).
482 Soil Biology & Biochemistry 104, 218-225.
483 Schnell, S., King, G.M., 1994. Mechanistic analysis of ammonium inhibition of atmospheric methane
484 consumption in forest soils. Applied and Environmental Microbiology 60, 3514-3521.

485 Sexstone, A.J., Revsbech, N.P., Parkin, T.B., Tiedje, J.M., 1985. Direct measurement of oxygen
486 profiles and denitrification rates in soil aggregates. Soil Science Society of America Journal 49,
487 645-651.
488 Shukla, P.N., Pandey, K.D., Mishra, V.K., 2013. Environmental determinants of soil methane
489 oxidation and methanotrophs. Critical Reviews in Environmental Science and Technology 43,
490 1945-2011.
491 Singh, B.K., Tate, K.R., Kolipaka, G., Hedley, C.B., Macdonald, C.A., Millard, P., Murrell, J.C.,
492 2007. Effect of afforestation and reforestation of pastures on the activity and population dynamics
493 of methanotrophic bacteria. Applied and Environmental Microbiology 73, 5153-5161.
494 Smith, K.A., Dobbie, K.E., Ball, B.C., Bakken, L.R., Sitaula, B.K., Hansen, S., Brumme, R., Borken,
495 W., Christensen, S., Prieme, A., Fowler, D., Macdonald, J.A., Skiba, U., Klemedtsson, L.,
496 Kasimir-Klemedtsson, A., Degorska, A., Orlanski, P., 2000. Oxidation of atmospheric methane in
497 Northern European soils, comparison with other ecosystems, and uncertainties in the global
498 terrestrial sink. Global Change Biology 6, 791-803.
499 Spohn, M., Giani, L., 2011. Impacts of land use change on soil aggregation and aggregate stabilizing
500 compounds as dependent on time. Soil Biology & Biochemistry 43, 1081-1088.
501 Stiehl-Braun, P.A., Hartmann, A.A., Kandeler, E., Buchmann, N., Niklaus, P.A., 2011a. Interactive
502 effects of drought and N fertilization on the spatial distribution of methane assimilation in
503 grassland soils. Global Change Biology 17, 2629-2639.
504 Stiehl-Braun, P.A., Powlson, D.S., Poulton, P.R., Niklaus, P.A., 2011b. Effects of N fertilizers and
505 liming on the micro-scale distribution of soil methane assimilation in the long-term Park Grass
506 experiment at Rothamsted. Soil Biology & Biochemistry 43, 1034-1041.
507 Tate, K.R., Ross, D.J., Saggar, S., Hedley, C.B., Dando, J., Singh, B.K., Lambie, S.M., 2007. Methane
508 uptake in soils from *Pinus radiata* plantations, a reverting shrubland and adjacent pastures:
509 Effects of land-use change, and soil texture, water and mineral nitrogen. Soil Biology &
510 Biochemistry 39, 1437-1449.
511 Wei, X.R., Li, X.Z., Jia, X.X., Shao, M.G., 2013. Accumulation of soil organic carbon in aggregates
512 after afforestation on abandoned farmland. Biology and Fertility of Soils 49, 637-646.
513 Wieczorek, A.S., Drake, H.L., Kolb, S., 2011. Organic acids and ethanol inhibit the oxidation of
514 methane by mire methanotrophs. FEMS Microbiology Ecology 77, 28-39.
515 Wilcke, W., Kretzschmar, S., Bundt, M., Zech, W., 1999. Metal concentrations in aggregate interiors,
516 exteriors, whole aggregates, and bulk of Costa Rican soils. Soil Science Society of America
517 Journal 63, 1244-1249.
518 Wu, Y.H., Zhang, H.J., Lv, W.X., Cheng, J.H., Wang, H.Y., 2013. Characteristics and aggregate
519 stability of soil particle size distribution under four forestland types in low mountains and hills of
520 Southwest China. Journal of Food Agriculture & Environment 11, 850-857.
521